



Thermal behaviour of kaolinitic raw materials from San José (Oruro, Bolivia)

P. Alfonso¹ · L. A. Penedo¹ · M. García-Valles² · S. Martínez² · A. Martínez¹ · J. E. Trujillo³

Received: 25 July 2021 / Accepted: 21 January 2022
© The Author(s) 2022

Abstract

Kaolin is widespread as a result of the alteration in the San José Sn-Ag deposit located in Oruro, Bolivia. This study presents a chemical, mineralogical and thermal characterization of the San José kaolinitic deposit, which is necessary to determine their optimal applications. Mineral phases of these white silty kaolinitic materials were determined by X-ray diffraction (XRD) and are quartz, kaolinite, K-feldspar, muscovite, illite and minor halloysite, dickite, plagioclase, jarosite, rutile, alunite and gypsum. The fraction < 63 µm contains 20–27 mass% of kaolinite. Differential thermal analysis (DTA) shows an endothermic peak at 520 °C associated with the dehydroxylation of kaolinite and an exothermic peak at ~980 °C related to the crystallization of mullite. TG curves show a total mass loss up to 1300 °C of about 8 mass%. The dilatometric curves show a shrinkage at about 890 °C produced by the collapse of metakaolinite into a spinel-like structure, and another shrinkage starts at 1010 °C, at the beginning of the sintering, when the spinel-like phase is transformed to mullite and amorphous SiO₂. Lightness L* is 80–92, but only the mined materials have b* < 4, suitable for paper filling applications.

Keywords Kaolin · Bolivia · X-ray diffraction · Thermal analysis · CIELab colour

Introduction

A significant source of primary kaolin comes from the alteration of host rocks produced during the circulation of hydrothermal fluids responsible to the formation of metallic deposits [1, 2]. Bolivia is known by its abundant metallic mineral resources. The abundant hydrothermal activity that formed most of the ore deposits in the Central Andean Tin Belt produced alteration of the host rocks that constitute important clay resources. Other kaolinitic deposits are related to degradation of materials of Devonian age in Bolivia [3]. They are also abundant in the tropical regions of the east part of the country, where they formed from supergene processes, such as the active exploitations of kaolin in the departments of Santa Cruz [4] and Cochabamba [5, 6].

The aim of this study is to present a mineralogical and thermal characterization of kaolinitic rocks located in the vicinity of the San José mine (Oruro, Bolivia) to determine their possible industrial applications. This kaolinitic area was formed as result of the alteration of volcanic rocks by hydrothermal fluids during the formation of the San José ore deposit. The mineralogical and thermal characterization of these kaolinitic materials have not been previously reported. A description of the area and mineralogy of the San José mine was reported by Keutsch and Brodtkorb [7]. An economic valuation of the exploitation of this deposit indicated the occurrence of 318,892 tons of kaolinitic material in this deposit [8].

The characterization of the kaolinitic materials is necessary to select the most suitable application. Traditionally kaolins have a wide number of uses, which depend on their composition and properties, the morphology, particle size distribution and colour are especially important for the final application [9]. The most important uses are in paper making, paints and ceramic uses, but also is used in the industry of rubber, plastics, pharmaceuticals, ink, catalysis, fibre glass and Portland cement [10]. The interest in kaolin has increased with the possibility to be used in the production of a cementitious material that can substitute the Portland

✉ P. Alfonso
maria.pura.alfonso@upc.edu

¹ Department d'Enginyeria Minera, Industrial i TIC, Universitat Politècnica de Catalunya, Manresa, Spain

² Department Mineralogia, Petrologia i Geologia Aplicada, Universitat de Barcelona, Barcelona, Spain

³ Facultad Nacional de Ingeniería, Universidad Técnica de Oruro, Oruro, Bolivia

cement and in this way contributing to reduce the emissions of CO₂ [11].

Material and analytical methods

Samples

Ten samples were obtained along the deposit located close to the San José-Itos mine. Two of them (SJ-1 and SJ-2) are representative samples of a quarry area that is been mined; the other samples belong to outcrops located in the surroundings of the quarry and do not were exploited. This area is located in the North part of the Oruro city, Bolivia, Central Andean Tin Belt. The clays which are the main subject of this study are formed from the hydrothermally altered magmatic-volcanic rock complex of the San José deposit, Oruro. Advanced argillitic alteration is widespread in the surroundings of this deposit with abundant kaolinitization.

Analytical methods

The particle size distribution of kaolins has been determined by a LS 13 320 Beckman Coulter particle size analyser. Samples were treated with sodium pyrophosphate and agitated mechanically for 24 h to achieve a total disaggregation. The samples were separated in different size fractions in order to determine where is the main clay concentration. In this process the 50 g of particles < 60 µm were introduced in 1L of a solution with deflocculant; particles between 2 and 20 µm were removed by sedimentation and the particles < 2 µm were separated filtering the solution.

The chemical composition of major elements of the kaolinitic materials was determined by X-ray fluorescence (XRF) using a sequential X-Ray spectrophotometer Philips PW 2400.

The mineralogy was determined by X-Ray Powder diffraction (XRPD) using random and oriented aggregates prepared following standard XRD procedures [12], which include three spectra of samples without treatment, glycolated with ethylene glycol and heated at 550 °C. The diffractograms were obtained from powdered samples in a Bragg–Brentano PANAnalyticalX’Pert Diffractometer system (graphite monochromator, automatic gap, K α -radiation of Cu at $\lambda = 1.54061$ Å, powered at 45 kV–40 mA, scanning range 4–100 ° with a 0.017 ° 2 θ step scan and a 50 s measuring time). Identification and semiquantitative evaluation of phases was made on PANAnalyticalX’Pert HighScore software. The Inorganic Crystal Structure Database (ICSD) was used for the mineral identification. Additionally, Fourier-transform infrared (FTIR) spectra were obtained using a PerkinElmer System 2000 FTIR spectrometer. Vibrational spectra were obtained in the 400–4000 cm⁻¹ range.

Electron scanning microscopy (SEM) equipped with an energy dispersive X-ray spectrometer (EDS) was used to observe the textures and morphology. The equipment used was a Hitachi TM-1000 table-top.

Thermal properties were determined by simultaneous differential thermal analysis and thermogravimetry (DTA-TG) and dilatometry. DTA-TG analyses were carried out using a STA 409C Netzsch equipment. Analyses were carried in a dry air atmosphere with a flux of at 80mLmin⁻¹ constant flow ratio. Samples of 83.5 mg were introduced in an alumina crucible and heated from 25 to 1300 °C with a linear rate of 10 °Cmin⁻¹, followed by free cooling. Aluminium oxide PerkinElmer 0419–0197 is taken as reference. Dilatometric analysis was measured by a Linseis horizontal dilatometer L76/1550. Samples were heated up to 1300 °C at a 10 °Cmin⁻¹ in a dry air atmosphere.

Colour was determined by the spectral diffuse reflectance in the CIELAB colour space [13]. The parameters were measured using a CM-700d Konica-Minolta spectrophotometer. The description of the colour was based on three parameters: lightness (L*), saturation (C*) and intensity (h_{ab}) [14], which were established from three coordinates, L*, a* and b*. L* indicates lightness, 100 being white colour and 0 black; a* and b* are the chromatic coordinates: +a* is the red axis, –a* is the green axis, +b* is the yellow axis and –b* is the blue axis.

The whiteness index (WI) was calculated using the equation of Stensby (1) [15, 16]

$$WI = L^* - 3b^* + 3a^* \quad (1)$$

where L*, b* and a* are the CIELAB parameters.

Results and discussion

Particle size distribution and morphology

Particle size is an important parameter in the properties of kaolin and has to be taken into account in the fabrication of ceramics [17]. The cumulative particle size distribution of the kaolinitic materials from San José is shown in Fig. 1. Fifty per cent (50%) of the materials (P₅₀) shows a particle size smaller than 5 µm and 80% of the particles (P₈₀) are smaller than 18 µm. The fraction < 2 µm represents 28% of all the materials.

The morphology of kaolinite provides useful information for the identification. All the kaolinite-group minerals have similar structure and composition, which makes difficult it to distinguish them [18] Kaolinite occurs as isolated or stacked plates, whereas halloysite although can be present in different morphologies it is usually with tubular shape [19]. SEM observations show

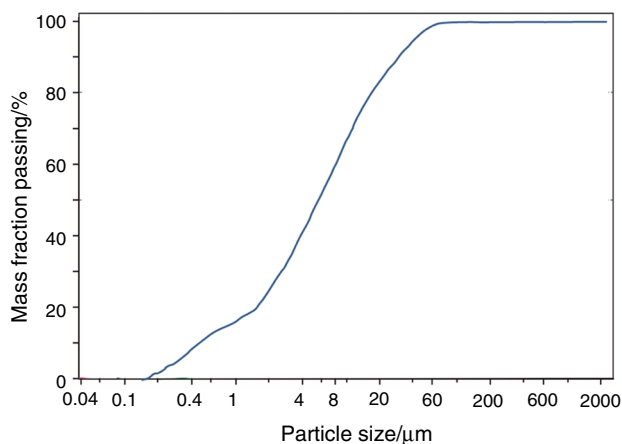


Fig. 1 Particle size distribution of the San José kaolinitic materials

that kaolin-group minerals from San José exhibit a platy regular morphology with hexagonal crystals of kaolinite, often grouped in stacks or in book-like shape (Fig. 2), whereas halloysite although can be present in different morphologies.

Chemical and mineralogical characterization

The main components of the kaolinitic materials from San José are SiO_2 (64 to 69 mass%), Al_2O_3 (19 to 20 mass%) and K_2O (4.03 to 5.51 mass%). In addition, there are minor amounts of Fe_2O_3 (0.61 to 1.11 mass%) and TiO_2 (up to 0.64 mass%) and Na_2O , CaO , MgO and P_2O_5 occur in lesser amounts (Fig. 3).

Fig. 2 Scanning electron microscopy images of San José. **a** Book aggregate of kaolinite, **b** presence of halloysite with tubular shape

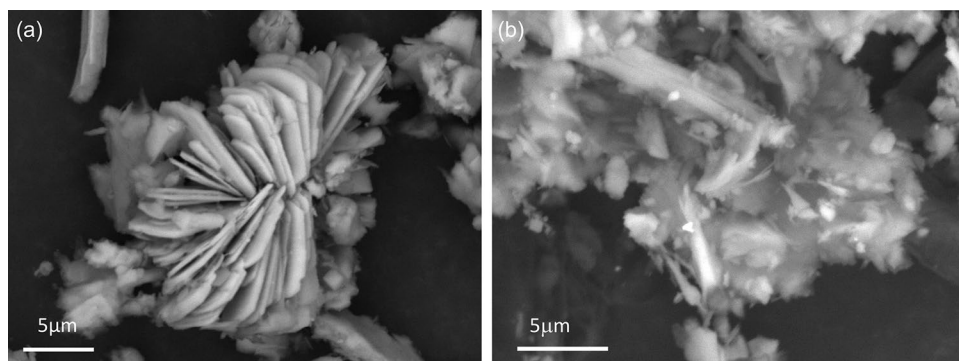
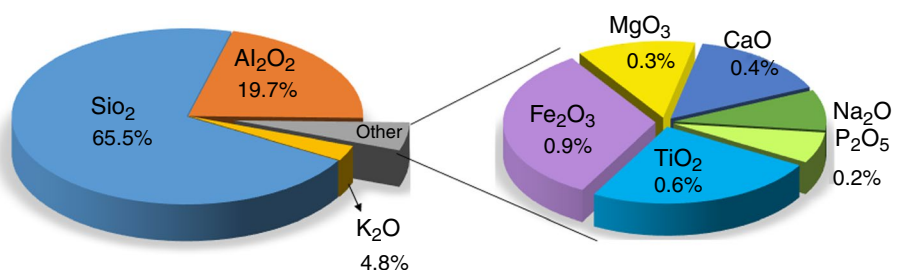


Fig. 3 Chemical composition of the San José kaolinitic materials



The mineralogical composition of these materials is presented in Table 1. The mineral phases are mainly quartz, K-feldspar, muscovite/illite plagioclase, kaolinite, halloysite and minor alunite, jarosite and gypsum. XRD from oriented aggregates (Fig. 4) confirm these clays identification. In some cases, instead of kaolin the kaolinite-group mineral dickite was identified. Dickite is especially formed during hydrothermal alteration of volcanic host rocks [19, 20]. In the San Pablo mine, located in the Central Andean Tin Belt, also dickite was reported [21].

The mineralogical analysis in particle size fractions reveal that most kaolinite is in the smaller fractions. The fraction $< 63 \mu\text{m}$ contains from 20 to 27 mass% of kaolinite and that between 2 and 20 μm has from 10 to 17 mass% kaolinite (Fig. 5). The same behaviour is followed by illite, whereas quartz and feldspar show the opposite behaviour (Table 2).

The FTIR spectrum of the San José kaolin (Fig. 6) shows the representative vibrations of kaolinite, associated to structural bonds of Si–O, Al–O, Al–OH, $\text{SiO}_4\text{--Al}_2\text{O}_3$ and Si–O–Al [22, 23]. In the region from 3800 to 3600 cm^{-1} the most characteristic absorption bands of kaolinite correspond to structural water and Al–OH stretching vibrations. These characteristic bands appear at 3698, 3673, 3650 and 3623 cm^{-1} . The theoretical doublet at 3694 and 3619 cm^{-1} , which in San José appears at 3698 and 3623 cm^{-1} , reveals a well-ordered kaolinite structure [22]. Bands at 1113, 1030 and 994 cm^{-1} correspond to Si–O stretching, a band at 920 cm^{-1} is attributed to Al–OH bending vibrations and at 790 and 765 cm^{-1} are attributed to OH deformation [22].

Table 1 Semiquantitative mineralogical composition, in mass%, of the San José kaolinitic materials. Kfs, K-feldspar; Pl, plagioclase; Ms, muscovite. Hyphen: under the detection limit

	Quartz	Kfs	Pl	Kaolinite	Dickite	Illite/Ms	Jarosite	Alunite	Rutile	Gypsum
SJ-1	59	6	–	7	–	24	–	2	–	2
SJ-2	40	18	9	8	–	21	–	4	–	–
SJ-18	56	7	5	8	–	24	–	–	–	–
SJ-19	47	7	–	6	–	37	2	–	–	–
SJ-20	66	3	–	–	8	21	2	–	–	–
SJ-21	61	5	–	4	–	27	2	–	–	–
SJ-22	56	8	4	10	–	20	–	–	1	–
SJ-24	55	11	–	11	–	22	1	–	–	–
SJ-62	52	17	–	–	8	19	–	4	–	–
SJ-63	68	6	–	5	–	21	1	–	–	–

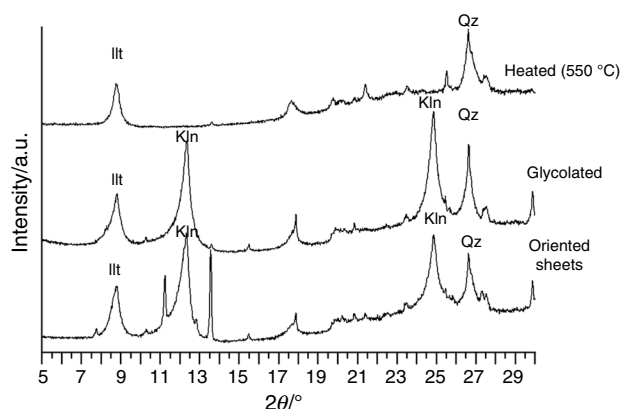


Fig. 4 Oriented aggregates XRD Patterns (sample Sj-2), treated with ethylene glycol and heated 550 °C. Qz, quartz; Ill, illite, Kln, kaolinite

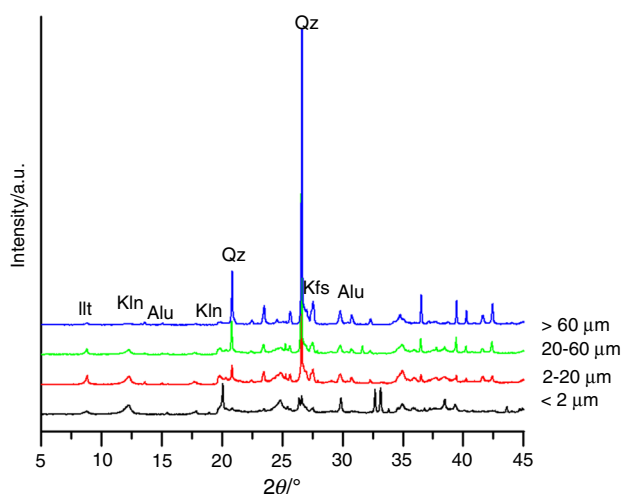


Fig. 5 XRD Patterns of the size fractions of the kaolinitic material of San José in a representative sample (Sj-2). Quartz Qz, Kfs, K-feldspar; Ill, illite; Kln, kaolinite and Alu, alunite

Table 2 Semiquantitative mineralogical composition, in mass%, the San José kaolinitic materials distributed in size fractions (sample SJ-1)

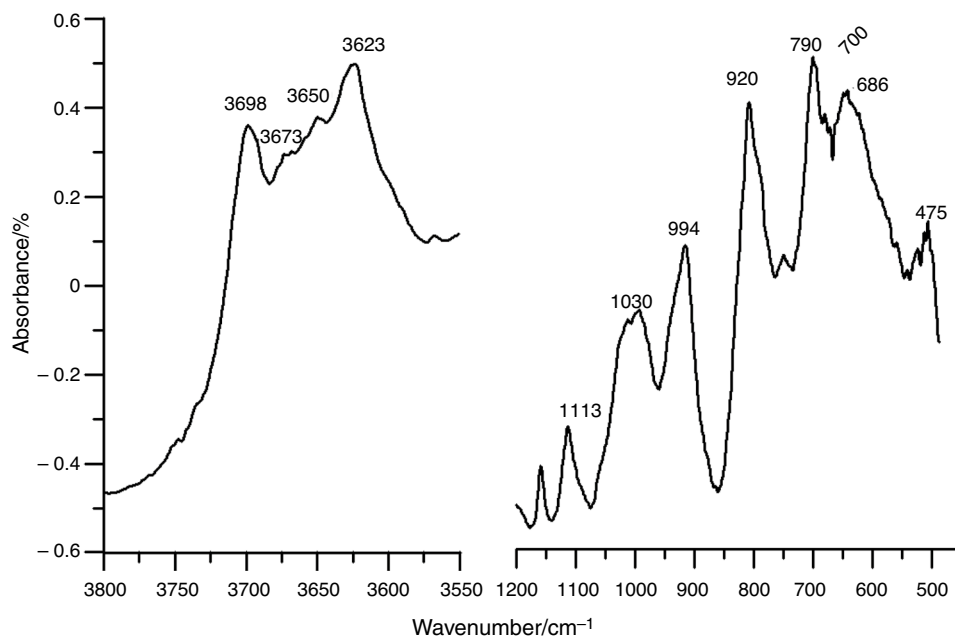
Fraction size (μm)	<2	2–20	20–60	>60
Quartz	8–19	25–34	51–53	56–63
K-feldspar	16–18	16–25	9–13	5–23
Kaolinite	20–28	10–17	10	8
Illite/Ms	36–41	25–26	20–24	12–21
Alunite	5–9	4–12	4–5	3

Thermal properties

Thermogravimetric analysis shows two steps of mass loss. The first step produces a mass loss of about 0.4 mass% and occurs in the range 25–200 °C and corresponds to adsorbed and interlayer water removal ascribed to kaolinite and illite. This change can be observed as an endothermic event shown in the first derivate curve (Fig. 7). The main mass loss, of about 6 mass%, occurs between 200 and 1200 °C and is related to the main DTA event, which is attributed to kaolinite dehydroxylation.

DTA shows an endothermic peak at 520 °C, caused by the release of clay OH⁻ groups and exothermic peak at ~980 °C related to the formation of a spinel-like phase and mullite from the destabilization of metakaolinite (Fig. 7). The temperature of the endothermic peak is related to the degree of order of kaolinite. According to Smykatz-Kloss [24] the endothermic lower than 530 °C corresponds to extremely disordered kaolinite. The halloysite content could also contribute to lower this peak, thus halloysite endothermic occurs at temperatures lower than 500 °C [25]. In the present study, the illite content is higher than kaolinite, contributing also to the endothermic event. However, the illite dehydroxylation occurs at higher temperature than kaolinite [26, 27].

Fig. 6 Representative FTIR spectrum of the San Jose kaolinitic materials (sample Sj-1)



The dilatometric analyses show the expansion–shrinkage evolution of all the phases in the material during heating and cooling processes, being mainly significant the effect of clays and quartz [27]. The dilatometric curves of the kaolinitic materials from San José are shown in Fig. 8. Firstly, with the increase of temperature up to 400 °C the expansion is slow. A more pronounced dilatation occurs between 500 and 520 °C attributed to the endothermic reaction of kaolinite, which is associated with the loss of structural OH^- groups. It is followed by a significant shrinkage at 500–600 °C due to the α - β polymorphic transformation of quartz at 573 °C. Another contraction is observed in the range 880–980 °C associated with the collapse of metakaolinite into a spinel-like structure. Recrystallization starts at 950–980 °C and causes a

reduction in the shrinkage, which reaches approximately up to 1010 °C, when the spinel-like phase is transformed to mullite and amorphous SiO_2 [23]. At higher temperatures there is a new shrinkage associated with the sintering. Finally, at 573 °C a polymorphic transformation of β - α quartz is reflected in the cooling curve. The lowest shrinkage occurs in the samples with lower quartz contents (Fig. 8). These samples are the alunite-richest. Alunite and jarosite have an influence in the shrinkage attributed to the release of their water molecules and SO_3 [28, 29].

XRD of the pieces used for the dilatometric tests, which were heated at 1300 °C show that the mineralogical composition after firing is quartz, mullite and a minor amount of rutile and occasionally hematite.

Fig. 7 DTA-TG curves (sample Sj-2.). The first derivate of the DTA curve (DDTA) is indicated with a dashed line

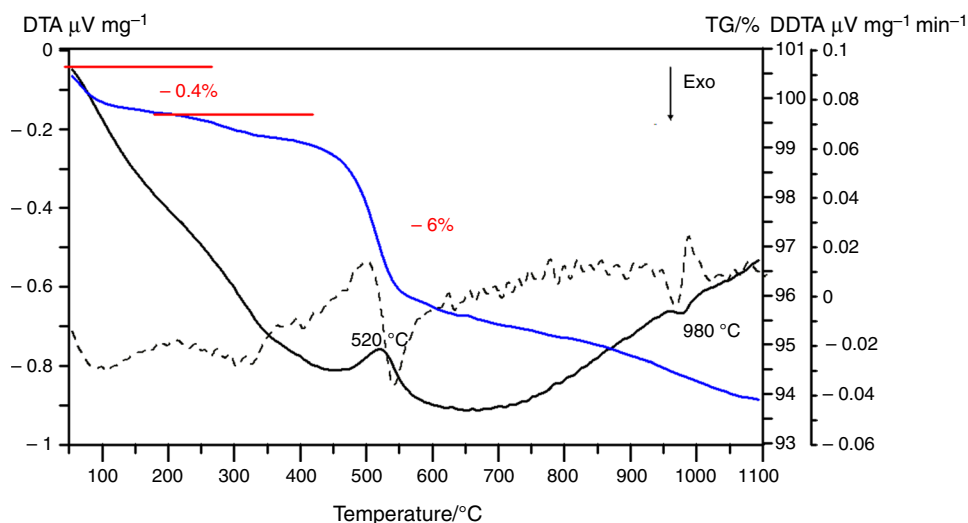
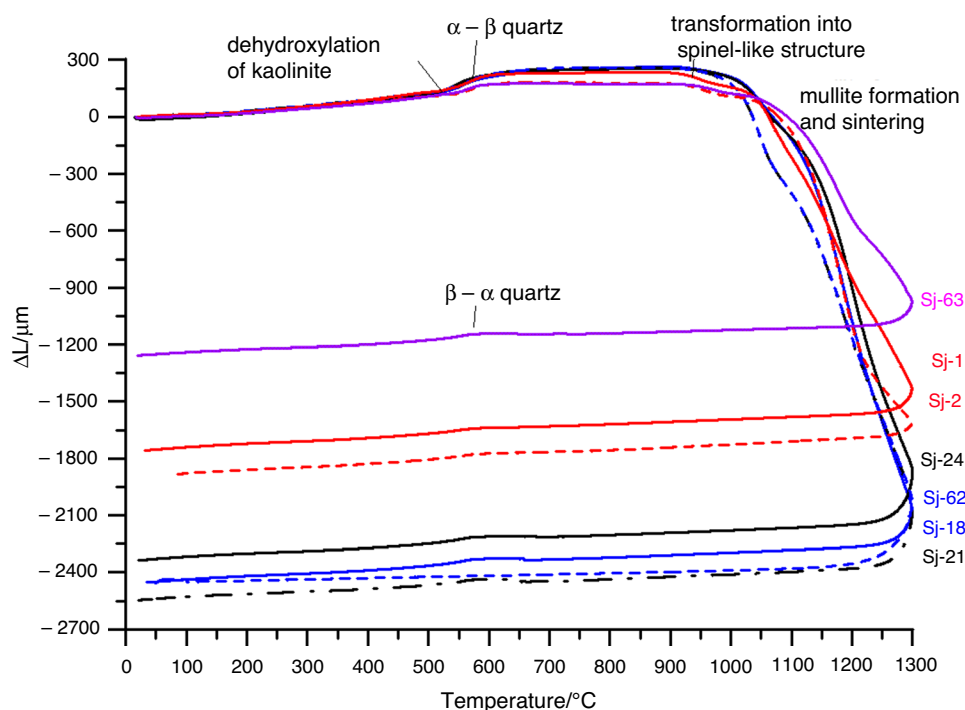


Fig. 8 Dilatometric curves of the kaolinitic materials from San José



Colour

The San José kaolinitic material vary from white to creamy (Fig. 9). The CIELAB parameters are shown in Table 3. Lightness control the possible applications of kaolin. The highest requirements are for the paper coating industry, which requires 81.5 to 90.5 of lightness [30]. Lightness is function of the particle size and particle size distribution [31]. The San José materials have a high value of lightness. However, the whiteness considerably varies; the lower whiteness is from samples with small amounts of jarosite ($\text{KFe}^{3+}_3(\text{SO}_4)_2(\text{OH})_6$), the iron content of this mineral is responsible of colour.

The exploited kaolinitic materials display highest whiteness in comparison with other samples collected in this area.

The colour depends on the mineralogical and chemical composition of the kaolinitic material, being the chromophore elements, mainly Fe^{3+} and Ti^{4+} [32, 33]. The redness (a^*) and yellowness (b^*) are inversely correlated to the lightness and whiteness (Fig. 10), being only the materials of the exploitation area with b^* low enough for specific uses as paper coatings, which requires a yellowness lower that 4.8 [30].

The chroma parameter (C^*) shows a negative correlation with L^* , but in the fired materials both have a slightly positive correlation. The h_{ab} parameter has a positive correlation with L^* in all the kaolinitic materials.

Fired pieces always show a decrease of lightness and whiteness with respect to the original kaolinitic materials (Table 3). The a^* parameter is similar to the darkest raw

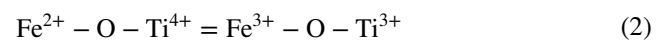


Fig. 9 Image of the kaolinitic materials powders

Table 3 Colour parameters of the San José kaolinitic materials

Samples	Kaolinitic powder	Fired materials (1300 °C)											
		L	a*	b*	C*	h _{ab}	WI	L	a*	b*	C*	h _{ab}	WI
SJ-1	92	-0.31	4.84	4.85	94	77							
SJ-2	92	0.09	4.27	4.27	89	80							
SJ-18	85	2.01	12.21	12.37	81	54	66	2.84	7.05	7.60	68	53	
SJ-19	83	3.54	16.14	16.52	78	45							
SJ-20	83	2.91	13.01	13.33	77	53	59	3.21	6.88	7.59	65	48	
SJ-21	82	3.89	14.37	14.89	75	51	61	3.57	6.67	7.56	62	52	
SJ-22	84	2.24	12.70	12.90	80	52	71	3.76	8.74	9.51	67	56	
SJ-24	83	2.00	12.31	13.20	77	53	62	3.97	8.19	9.08	64	50	
SJ-62	90	0.54	5.11	5.14	84	77	81	2.54	8.85	9.21	74	62	
SJ-63	88	0.88	7.48	7.53	83	68	83	2.72	10.33	10.68	75	60	

kaolinitic materials and do not follow is not correlated with the lightness, whereas b^* of the fired pieces is lower than in hematite- rutile-bearing samples; a similar relationship occurs between lightness and the C^* parameter (Fig. 10d). The lack of correlation between lightness and a^* , b^* and C^* in the heated materials could be attributed to the different mineral transformations. Part of Fe in the natural kaolinitic material can be as Fe^{2+} located in the structure of rutile in substitution of Ti^{4+} . In this case, during the heating Fe^{2+} gives off one electron to Ti^{4+} and becomes Fe^{3+} [34], following the reaction (2) presented by Hogg and Noble [35]:

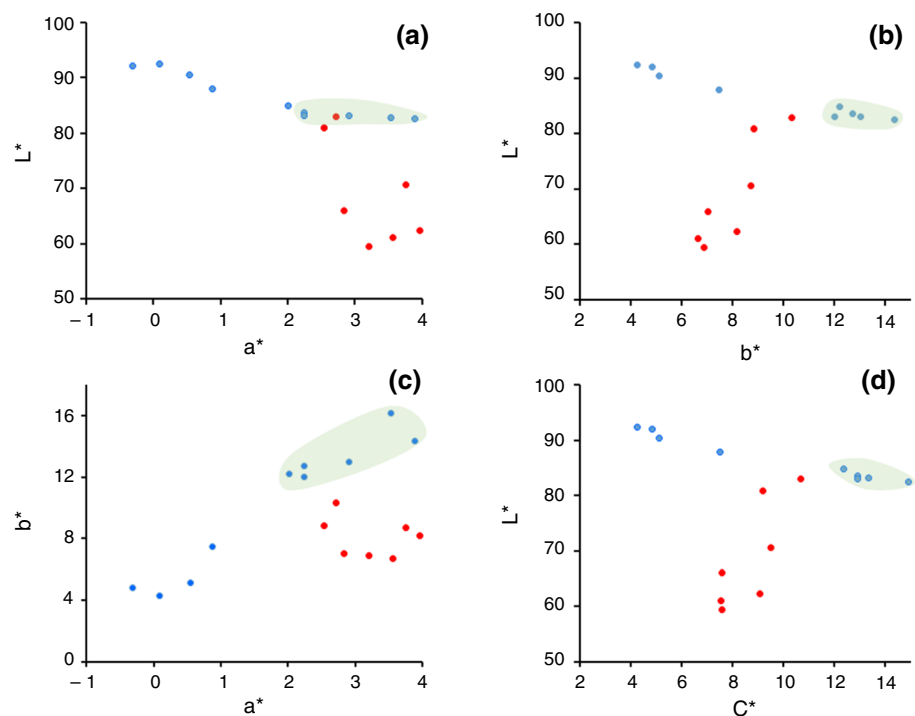


As a consequence, the crystallization of hematite is produced.

Conclusions

The mineralogy of the San José kaolinitic materials, with high amount of quartz, suggests that the main application for these clays should be in the field of ceramics. Kaolinite is highly concentrated in the $< 2 \mu m$ fraction it reach values between 20 and 28 mass% of the total and clays represent 61–78 mass%. Then, with an enrichment process there could

Fig. 10 Plots showing the relationships of the CIELAB parameters. Blue dots, natural kaolinitic materials, red dots, fired materials. Green area indicates natural samples containing hematite or rutile. **a** a^* vs L^* , **b** b^* vs L^* , **c** a^* vs b^* , **d** C^* vs L^*



be many other applications favoured by its low iron content, usually lower than 1.1 mass% Fe₂O₃.

Usually, these kaolins exhibit relatively low shrinkage (about 8 mass%), which makes them suitable for the ceramic applications. The α - β transformations of the silica minerals during the firing process produce expansions and shrinkages in the ceramic pieces. Thus, the content of these minerals must be controlled and also the rate of increase of temperature during firing.

Other areas located near the mined quarry of San José are also rich in kaolinite or dickite, being locally richer, up to 11 mass% of kaolinite.

Acknowledgements This research was financed by the projects 2016-U006 and 2020-B006 funded by the Centre de Cooperació al desenvolupament de la UPC (CCD) and the 2017SGR1687 and 2017SGR0707 projects (Generalitat de Catalunya).

Author contributions MG and P.A. wrote the paper; JET, PA and LAP did the field work, MG and LAP did the laboratory work; SM Assisted with the interpretation of results. AM assisted with production of images and writing. All authors contributed to data interpretation and discussion.

Funding Open Access funding provided thanks to the CRUE-CSIC agreement with Springer Nature. This research was financed by the projects 2016-U006 and 2020-B006 funded by the Centre de Cooperació al desenvolupament de la UPC (CCD) and the 2017SGR1687 and 2017SGR0707 projects (Generalitat de Catalunya).

Declarations

Conflict of interest All the authors declared that they have no conflicts of interest.

Consent to participate All authors agree with the content and all gave consent to submit this manuscript.

Consent for publication All authors gave their permission of publication.

Open Access This article is licensed under a Creative Commons Attribution 4.0 International License, which permits use, sharing, adaptation, distribution and reproduction in any medium or format, as long as you give appropriate credit to the original author(s) and the source, provide a link to the Creative Commons licence, and indicate if changes were made. The images or other third party material in this article are included in the article's Creative Commons licence, unless indicated otherwise in a credit line to the material. If material is not included in the article's Creative Commons licence and your intended use is not permitted by statutory regulation or exceeds the permitted use, you will need to obtain permission directly from the copyright holder. To view a copy of this licence, visit <http://creativecommons.org/licenses/by/4.0/>.

References

- Murray HH. Kaolin minerals: their genesis and occurrences. In: Bailey SW, editor. *Hydrous phyllosilicates (Exclusive of micas)*. Washington, D.C.: Reviews in Mineralogy; Mineralogical Society of America; 1988. p. 67–89.
- Dill HG. Kaolin: soil, rock and ore: from the mineral to the magmatic, sedimentary and metamorphic environments. *Earth-Sci Rev.* 2016;161:16–29.
- Zeballos A, Weihed P, Blanco M, Machaca V. Geological, mineralogical and chemical characterization of Devonian kaolinite-bearing sediments for further applications in the ceramic (tiles) industry in La Paz. *Bolivia Environ Earth Sci.* 2016;75:546.
- Zeballos A, Weihed P, Blanco M, Machaca V. Characterization of some nonmetallic resources in Bolivia: an overview of their potentiality and their application in specialized formulations. *Environ Earth Sci.* 2017. <https://doi.org/10.1007/s12665-017-7094-7>.
- Escalera E, Antti ML, Odén M. Thermal treatment and phase formation in kaolinite and illite based clays from tropical regions of Bolivia. *IOP Conf Ser: Mater Sci Eng.* 2012;31:012017. <https://doi.org/10.1088/1757-899X/31/1/012017>.
- Escalera E, Tegman R, Antti ML, Odén M. High temperature phase evolution of Bolivian kaolinitic–illitic clays heated to 1250° C. *Appl clay sci.* 2014;101:100–5.
- Keutsch F, de Brodtkorb MK. Metalliferous paragenesis of the San José mine, Oruro Bolivia. *J S Am Earth Sci.* 2008;25:485–91.
- Medinaceli Torrez R, Trujillo LE. Estudio técnico y económico de la explotación del yacimiento de Caolín perteneciente a la Carrera de Ingeniería de minas, petróleo y geotecnia de la UTO. *Rev de Medio Ambiente y Minería.* 2016;1:46–55.
- Prasad MS, Reid KJ, Murray HH. Kaolin: processing, properties and applications. *Appl clay sci.* 1991;6:87–119.
- Murray HH. Kaolin Applications. In: *Developments in clay science*. Elsevier; 2006. p. 85–109.
- Flores Segura JC, Reyes Cruz VE, Pérez Bueno JJ, Lozada Ascencio EM, Legorreta García F. Characterization and electrochemical treatment of a kaolin. *Appl Clay Sci.* 2017;146:264–9.
- Moore DM, Reynolds RC Jr. *X-ray Diffraction and the Identification and Analysis of Clay Minerals*. 2nd ed. New York: Oxford University Press; 1997.
- CIE. Technical report, colorimetry. *Commission Internationale de L'Eclairage*, 1931.
- Mokrzycki WS, Tatol M. Colour difference ΔE -A survey. *Mach Graph Vis.* 2011;20(4):383–411.
- Stensby PS. Optical brighteners as detergent additives. *J Am Oil Chem Soc.* 1968;45(7):497–504. <https://doi.org/10.1007/BF02541335>.
- Pi-Puig T, Animas-Torices DY, Solé J. Mineralogical and geochemical characterization of talc from two Mexican ore deposits (Oaxaca and Puebla) and nine talcs marketed in Mexico: Evaluation of its cosmetic uses. *Minerals.* 2020;10(5):388.
- Hubadillah SK, Harun Z, Othman MHD, Ismail AF, Gani P. Effect of kaolin particle size and loading on the characteristics of kaolin ceramic support prepared via phase inversion technique. *J Asian Ceram Soc.* 2016;4(2):164–77.
- Joussein E, Petit S, Churchman J, Theng B, Righi D, Delvaux B. Halloysite clay minerals—a review. *Clay min.* 2005;40:383–426.
- Nagasawa K. Kaolin minerals. In: *Developments in sedimentology*. Elsevier; 1978. p. 189–219.
- Choo CO, Kim SJ. Dickite and other kaolin polymorphs from an Al-rich clay deposit formed in volcanic tuff, southeastern Korea. *Clay Clay Miner.* 2004;52:749–59.
- Jiménez-Franco A, Alfonso P, Canet C, Trujillo JE. Mineral chemistry of In-bearing minerals in the Santa Fe mining district. *Bolivia Andean Geol.* 2018;45(3):410–32.
- Vaculíková L, Plevová E, Vallová S, Koutník I. Characterization and differentiation of kaolinites from selected Czech deposits using infrared spectroscopy and differential thermal analysis. *Acta Geodyn Geomater.* 2011;8(161):59–67.

23. Garcia-Valles M, Alfonso P, Martínez S, Roca N. Mineralogical and thermal characterization of kaolinitic clays from Terra Alta (Catalonia, Spain). *Minerals*. 2020;10(2):142. <https://doi.org/10.3390/min10020142>.
24. Smykatz-Kloss W. *Differential Thermal Analysis: Application and Results in Mineralogy*. Springer-Verlag; 1974.
25. Bordeepong S, Bhongsuwan D, Punggrassami T, Bhongsuwan T. Characterization of halloysite from Thung Yai District, Nakhon Si Thammarat Province in Southern Thailand. *Songklanakarin J Sci Technol*. 2011;33(5):559–607.
26. Fernandez R, Martirena F, Scrivener KL. The origin of the pozzolanic activity of calcined clay minerals: a comparison between kaolinite, illite and montmorillonite. *Cem Concr Res*. 2011;41:113–22.
27. Húlan T, Trník A, Kaljuvee T, Uibu M, Štubňa I, Kallavus U, Traksmaa R. The study of firing of a ceramic body made from illite and fluidized bed combustion fly ash. *J Therm Anal Calorim*. 2017;127(1):79–89.
28. Frost RL, Wain DL, Wills RA, Musumeci A, Martens W. A thermogravimetric study of the alunites of sodium, potassium and ammonium. *Thermochim Acta*. 2006;443:56–61.
29. Garcia-Valles M, Pi T, Alfonso P, Canet C, Martínez S, Jiménez-Franco A, Tarragó M, Hernández-Cruz B. Kaolin from Acoculco (Puebla, Mexico) as raw material: mineralogical and thermal characterization. *Clay Miner*. 2015;50(3):405–16.
30. Siddiqui MA, Ahmed Z, Saleemi AA. Evaluation of Swat kaolin deposits of Pakistan for industrial uses. *Appl Clay Sci*. 2005;29:55–72.
31. Bundy WM, Ishley JN. Kaolin in paper filling and coating. *Appl Clay Sci*. 1991;5:397–420.
32. Barba A, Beltrán V, Feliu C, García J, Ginés F, Sánchez E, Sanz V. *Materias primas para la fabricación de soportes de baldosas cerámicas*. Ed. Instituto de Tecnología Cerámica, 2002.
33. Bouzidi N, Siham A, Concha-Lozano N, Gaudon P, Janin G, Mahtout L, Merabet D. Effect of chemico-mineralogical composition on color of natural and calcined kaolins. *Color Res Appl*. 2014;39:499–505.
34. Chandrasekhar S, Ramaswamy S. Influence of mineral impurities on the properties of kaolin and its thermally treated products. *Appl Clay Sci*. 2002;21:133–42.
35. Hogg CS, Noble FR. A Kubelka–Munk analysis of the influence of iron and titanium oxides on the optical properties of hard porcelain. *Sci Ceram Berchtesgad Ger*. 1979;10:703–10.

Publisher's Note Springer Nature remains neutral with regard to jurisdictional claims in published maps and institutional affiliations.